Conditions for initial quasilinear T_2^{-1} versus τ for Carr-Purcell-Meiboom-Gill NMR with diffusion and susceptibility differences in porous media and tissues

Robert J. S. Brown
515 West 11th Street, Claremont, California 91711-3721

Paola Fantazzini
Dipartimento di Fisica, Università di Bologna, Via Irnerio 46, I-40126 Bologna, Italy
(Received 3 November 1992)

Porous media containing fluids and subject to the field of an NMR instrument usually have incremental local magnetic fields due to susceptibility differences χ_d, such as between a fluid and a solid matrix. If $|\chi_d| \ll 1$ the effective variation ω of the local precession angular frequency is limited to $\pm\frac{1}{2}\chi_d\omega_0$, where ω_0 is the mean precession angular frequency. Diffusion of fluid molecules through these local fields leads to a τ-dependent increase R_d in the value of $1/T_2$ obtained from Carr-Purcell-Meiboom-Gill (CPMG) measurements. Many porous media appear likely to have significant ω variation over a substantial range of diffusion time scales, or correlation times. For a sample with a single correlation time τ_c the logarithm of the additional decay of the nth echo amplitude due to diffusion through regions of different ω is $\Omega^2\tau_c\{2n\tau f(\tau/\tau_c)-\tau_c[(1-x)^4/(1+x^2)^2][1-(-)^n x^{2n}]\}$, where $f(t)=1-(\tanh t)/t$, $\Omega^2=\langle\omega^2\rangle$, and $x=\exp(-\tau/\tau_c)$. The term without n causes only a shift in the relaxation curve, and the terms in x^{2n} are small, so $R_d \approx \Omega^2\tau_c f(\tau/\tau_c)$. The function $f(t)$ starts quadratically at small t, has a nearly linear portion, and then approaches $1-1/t$ at large t. However, the superposition of terms of the form $f(\tau/\tau_{ci})$ tends to give a nearly linear portion of the R_d vs τ curve extending from small values of R_d to about a third of the asymptotic value if there is a significant range of τ_{ci}. For this linear portion the effect of a shift in all the τ_{ci}, such as from a change of temperature or from a liquid with a different diffusion coefficient, is small. Examples of measurements of T_1, of T_2 by Hahn single echoes, and of T_2 by CPMG measurements for a porous porcelain sample and a natural porous chalk sample illustrate this nearly linear τ dependence, which is quite different from the quadratic dependence for unrestricted diffusion in a uniform field gradient. The CPMG data were fit very well over the entire range by a function of the form $R_a+R_b\tan^{-1}(R_c\tau)$, and the computed asymptotes match the Hahn single-echo results for $\tau \gg \tau_c$ surprisingly well. Our result depends on the limited range of field variation and does not apply to the case of ferromagnetic or superparamagnetic grains in close contact with diffusing fluid molecules. Our approach can also be applied, under particular circumstances, to biological tissues.

INTRODUCTION

The surfaces of porous media have long been known to increase both longitudinal and transverse relaxation rates for nuclear magnetization in nuclear magnetic resonance (NMR) measurements of fluids in the pore spaces. The media have been as diverse as rocks, ceramics, plastic-fiber composites, plants, and biological tissues, which can, for our purposes, be considered to be porous media. Most of the early work relating NMR to fluid flow properties of porous media was done on longitudinal relaxation times T_1. However, one early application, the nuclear magnetism logging (NML) of oil wells[1] made the tentative identification of producible fluid on the basis of transverse relaxation times T_2. Not very much work has been done until more recently on T_2 behavior of fluids saturating porous media. A problem in the interpretation of the T_2 data has been that inhomogeneous fields of several sources other than the atomic- and molecular-scale effects cause transverse signal decay. For laboratory NMR, in the usual strong magnetic fields but without intentionally applied field gradients, the difference in magnetic susceptibilities[2-8] between the porous material and the pore fluid makes inhomogeneous magnetic fields in the pore spaces. These cause a transverse signal decay which may not be refocused in spin-echo measurements if diffusion of fluid molecules is rapid enough. This effect is also relevant in magnetic resonance microimaging.[9,10] The Carr-Purcell-Meiboom-Gill[11,12] (CPMG) measurement is often used to minimize the diffusion effects. Here trains of echoes spaced at intervals of 2τ are produced. If τ is sufficiently short that molecules in the fluid do not diffuse far enough in a time τ to change field and precession frequency significantly, then the echo decay curve represents transverse relaxation from the surface effects plus that of the bulk fluid. However, the distance for a significant change of field in some parts of the pore space may be so short that the shortest experimentally available τ values may not completely suppress the diffusion effects. For this reason various workers in both biological and nonbiological fields have made measurements at series of τ values and made extrapolations of various kinds[3,4,8,13] to $\tau=0$.

The transverse relaxation rate $1/T_2$ can be regarded as

the sum of the surface contribution R_s, the bulk fluid rate R_0, the rate difference $R_d(\tau)$ caused by diffusion in the inhomogeneous fields due to susceptibility differences in the porous medium, and in some cases still further mechanisms. In addition, there are usually inhomogeneous fields from the NMR instrument itself, but these are normally on a sufficiently large distance scale that diffusion does not interfere with the refocusing into echoes. Any or all of these sources of relaxation may lead to decay more complex than single exponential, that is, that cannot be described by a single relaxation time. For instance, many sandstone rocks have wide distributions of relaxation times even for T_1 or for CPMG T_2 measurements at very short τ values. Some of these materials are homogeneous to the eye and yet have different surface relaxation environments over very short distances, with sufficiently little mixing by diffusion in measurement times not to give a single uniform relaxation time. This does not mean that individual pores are in the "slow diffusion regime," but rather that the large pores do not mix with some of the smaller ones in measurement times. Some natural and artificial porous media[8] have given an initial linear τ dependence for various "average" relaxation times such as stretched exponential or geometric mean. Le Doussal and Sen[14] have recently shown that diffusion in a parabolic magnetic field leads to a linear τ dependence of $1/T_2$ from CPMG measurements.

In the present work we assume that this diffusion in the presence of field gradients due to susceptibility differences is the only source of dependence of $1/T_2$ on τ. However, Santyr, Henkelman, and Bronskill[15] have shown that the CPMG echo sequence can reduce $1/T_2$ to $1/T_{1\rho}$ at frequency $1/(4\tau)$. For systems that have significant T_1 dispersion below the maximum value of $1/(4\tau)$ for the data, an alternative[15] to the CPMG sequence is given.

Several approaches[3,13] to the extrapolation of $R_d(\tau)$ to $\tau=0$ have been based on the expression for the τ dependence of R_d in an unbounded homogeneous fluid in a uniform field gradient, $R_d(\tau)=(\gamma^2G^2D/3)\tau^2$, where γ is the magnetogyric ratio, G the field gradient, and D the diffusion constant. In some work an estimate of a typical value of some form of average of the gradient[2] in the porous medium is used for G. Therefore, $R_d(\tau)$ has been plotted against τ^2, but straight lines have not really resulted. The present problem differs from the uniform-gradient model in two ways. The gradient is quasiperiodic rather than uniform, and the diffusion is severely restricted by the porous medium.

MAGNETIC FIELDS FROM SUSCEPTIBILITY DIFFERENCES

Most porous media are too complex to be exactly described by mathematical models. An attempt will be made here to identify relevant features of these media and to find the consequences of these by approximate mathematical treatment. The aim is to understand the approximately linear dependence of $1/T_2$ on τ, which has been noted by Borgia *et al.*,[8] and to establish some limitations on the conditions for this to occur.

A central feature of the inhomogeneous magnetic fields in porous media resulting from differences of diamagnetic (or weak paramagnetic) susceptibilities between the solid matrix and a fluid in the pore spaces is that there is significant variation of fields or field gradients over a wide range of distance scales in different locations in the sample, including even within a single pore. Field gradients are most intense near sharp discontinuities in the pore system. In these regions diffusion over very small distances can bring a molecule to a different precession frequency and prevent the refocusing of part of the signal that would otherwise contribute to spin echoes. On the other hand, there is likely to be a region in the middle of a pore where the field is relatively uniform and where diffusion must occur over longer distances, and hence over longer times, to cause deterioration of contributions to spin echoes. It may be noted that a spherical or ellipsoidal cavity, with a different susceptibility from that of an infinite medium in which it is embedded, has no field gradient at all. It does, however, have a frequency shift, and in a porous rock a pore may have a different frequency from those of other pores or channels. Diffusion over pore size dimensions may be required before significantly different fields are encountered by molecules starting in the middle of such a pore. Diffusion over distances of pore spacings or more may play a part in CPMG echo train decay if T_2 is long enough.

We will first discuss some general geometrical features of porous systems, including biological tissues, and the related magnetic field differences $\mathbf{B}_d$ due to volume-susceptibility differences. For instance, diamagnetic susceptibility differences χ_d between quartz or calcite and water are of the order of 0.5×10^{-5} S.I. units (or a factor of 4π smaller in emu). This is so small that we may tentatively regard the magnetization difference between the solid and the fluid as everywhere in the solid phase equal to $\chi_d\mathbf{H}_0$, or $\chi_d\mathbf{B}_0/\mu_v$, where $\mathbf{H}_0$ and $\mathbf{B}_0$ are the main magnetic fields of the NMR instrument and $\mu_v=4\pi\times10^{-7}$ H per m is the permeability of free space. Thus, we neglect second-order terms representing magnetization due to the fields from the other magnetization, notwithstanding the existence of formal singularities to be discussed. That is, we are not discussing the channeling and concentration of flux as is done by high permeability magnetic circuits. Furthermore, we consider only B_d, the component of $\mathbf{B}_d$ parallel to $\mathbf{B}_0$, since this determines the precession frequency. There can, of course, be more components with different (but small) susceptibilities, and in media such as biological tissues there is not necessarily a solid component.

The contribution to $\mathbf{B}_d$ due to a dipole moment $(\chi_d\mathbf{B}_0/\mu_v)dV$ is given by

$$d\mathbf{B}_d=(-1/4\pi)\nabla(\chi_d\mathbf{B}_0\cdot\nabla)(1/r)dV\ .$$

Integrating over the solid framework of the porous medium, letting χ_d be constant, and letting $\hat{\mathbf{z}}$ be the unit vector in the direction of $\mathbf{B}_0$, we have

$$B_d=\frac{-\chi_dB_0}{4\pi}\int(\hat{\mathbf{z}}\cdot\nabla)(\hat{\mathbf{z}}\cdot\nabla)\left[\frac{1}{r}\right]dV$$

$$=\frac{-\chi_dB_0}{4\pi}\int\frac{\partial^2}{\partial z^2}\left[\frac{1}{r}\right]dV\ , \qquad (1)$$

where r is the radial distance from field point to source point, and dV is the contributing volume element. This may be converted into a surface integral,

$$B_d=\frac{-\chi_d B_0}{4\pi}\int\frac{\partial}{\partial z}\left[\frac{1}{r}\right]dS_z$$
$$=\frac{\chi_d B_0}{4\pi}\int\left[\frac{z_f-z_s}{r^3}\right]dS_z\ , \tag{2}$$

where the subscripts f and s indicate the field and source points, respectively, and dS_z is the projection of the surface element onto the x-y plane. In two dimensions we have the analogous expressions

$$B_d=\frac{\chi_d B_0}{4\pi}\int\frac{\partial^2}{\partial z^2}(-2\ln r)dS$$
$$=-\frac{\chi_d B_0}{2\pi}\oint\frac{z_f-z_s}{r^2}dy\ , \tag{3}$$

where y is the dimension normal to z, and the integral is around each solid area of the two-dimensional porous material. Note that for an element of surface that is normal to the z direction, the contribution to the integral in Eq. (2) is the element of solid angle subtended.

To see how to get the strongest B_d for a given χ_d and B_0 in a porous material, note that a contribution of a volume element is, in spherical polar coordinates, proportional to $(3\cos^2\vartheta-1)/r^3$. Contributions are positive if $|\cos\vartheta|>1/\sqrt{3}$. Thus, a cone of half-angle $\vartheta_0=\cos^{-1}\sqrt{1/3}\approx 55°$, or actually, two opposing cones of this angle, gives the maximum field at the apex. To study the behavior of this we can evaluate Eq. (2) to get the field at the apex of a single truncated right circular cone when $\mathbf{B}_0$ is parallel to the axis of the cone. The integrals for the plane surfaces at the top and bottom can be expressed in terms of angles, with lengths canceling, so these contributions cancel. If h is the distance along the slant edge, and ϑ is the half-angle, Eq. (2) gives

$$B_d=\frac{\chi_d B_0}{4\pi}\int_{h_1}^{h_2}\frac{(h\cos\vartheta)(2\pi h\sin\vartheta dh)\sin\vartheta}{h^3}$$
$$=\frac{\chi_d B_0}{2}\sin^2\vartheta\cos\vartheta\ln\frac{h_2}{h_1}\ . \tag{4}$$

We note that the field becomes infinite as $h_1\to 0$ or $h_2\to\infty$. If we regard our cone as a sharp point on the edge of a pore, we see that h_2 cannot be larger than some fraction of a pore radius; at larger radii the solid is seen at angles making negative as well as positive contributions. On the other hand, h_1 could be small down to atomic dimensions.

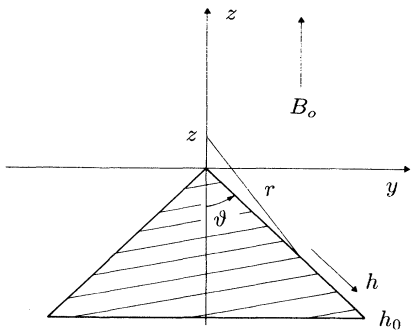

FIG. 1. The crosshatched area represents the section of either a cone or of a wedge of material of magnetic susceptibility slightly different from that of the surroundings. The slant height is h_0 and slant distance from the origin is h. The half-angle is ϑ, and the field is calculated at a point on the z axis.

As noted, we could double the above field by the unlikely geometry of two opposing cones. However, the related geometry with fluids in the opposing cones and with a narrow connecting cylindrical region near the apex gives the integral in Eq. (4) but with a factor of 2 and the opposite sign. This hourglass-shaped fluid region could be a channel connecting two pores. Thus, we have identified the geometries giving the strongest positive and negative local fields. As a function of h_1/h_2 these fields are not bounded, so we will investigate the consequences of the logarithmic singularities. To examine the nature and the consequences of the strong fields near the apex of the cone, we will compute the field on the axis of a right circular cone with a mathematically sharp point.

The geometry is shown in Fig. 1, and we let $\xi=z/h_0$, where h_0 is the slant height of the cone. There is rotational symmetry about the z axis, and the cross section represents a cone of susceptibility difference χ_d. We use Eq. (2) for this three-dimensional case to get

$$B_d=\frac{\chi_d B_0}{2}\left[\frac{\cos\vartheta(2\cos^2\vartheta-1)+\xi\cos^2\vartheta}{\sqrt{1+2\xi\cos\vartheta+\xi^2}}-\cos^2\vartheta+\cos\vartheta\sin^2\vartheta\ln\frac{\sqrt{1+2\xi\cos\vartheta+\xi^2}+1+\xi\cos\vartheta}{\xi(1+\cos\vartheta)}\right]. \tag{5}$$

For investigating the field in the vicinity of the singularity, it is convenient to expand Eq. (5) to first order in ξ,

$$B_d\approx\frac{\chi_d B_0}{2}\left[-\cos\vartheta(1-\cos\vartheta)(1+2\cos\vartheta)+\sin^2\vartheta\cos\vartheta\ln\frac{2}{1+\cos\vartheta}+3\xi\sin^2\vartheta\cos^2\vartheta-\sin^2\vartheta\cos\vartheta\ln\xi\right]. \tag{6}$$

We see a logarithmic singularity at the origin, and we now compute an upper limit to the dephasing effects of fields stronger than $\frac{1}{2}\chi_d B_0$ for the conical geometry. We integrate the rate of dephasing, originating near the origin of coordinates in Fig. 1, over volume out to the distance z_0 where $B_d=\frac{1}{2}\chi_d B_0$ and the angular frequency *difference* is $\omega=\frac{1}{2}\chi_d\omega_0$. Here ω_0 is the mean precession angular frequency of the signal-giving pore space. We assume, without specific computation, that B_d falls off with distances in various directions from the origin roughly as fast as along the z axis. The volume element at a distance r from the origin is proportional to r^2dr, so we evaluate $\int_0^{z_0} r^2\omega(r)dr$ and divide by $\int_0^a r^2dr$ out to an effective pore radius a, where ω is the incremental frequency due to our cone. We assume that h_0 is not more than half the effective pore radius a. For the coefficient of $\frac{1}{2}\chi_d B_0$ in Eq. (5) to equal 1.0, we need $1/\xi_0=h_0/z_0=40$, or $a/z_0=80$, using $\vartheta=\vartheta_0$ for the maximum effect. For a NMR frequency of 200 MHz and $\chi_d=0.5\times10^{-5}$, we get a rate of phase change of about 0.01 $\sec^{-1}$ for the entire pore space if there is full mixing by diffusion. The region for which $|\omega|>\frac{1}{2}\chi_d\omega_0$ is only one part in half a million of the pore volume, so, with no diffusion, signal loss from this region would be negligible. With diffusion the phase changes could, in a time of 1 sec, conceivably be spread more effectively to give a phase distribution with a width of the order of 0.01 rad, which would be negligible in most work. At lower NMR frequencies this would, of course, be less yet. Furthermore, this is an unrealistic "worst case," in which we have assumed the following three conditions: (1) Diffusion prevents any refocusing whatever to produce echoes for the magnetization involved. (2) There is no "averaging out" of phase dispersal. (3) There is no "overkill;" that is, no large amount of the phase dispersal is "wasted" on a small amount of magnetization.

In short, for practical purposes, one can ignore the singular contributions and regard the local magnetic field variations B_d, due to susceptibility variations $|\chi_d|\ll1$, from the local mean field in the pore spaces as limited to roughly $\pm\frac{1}{2}\chi_d B_0$, although, as we have seen, this can be doubled for a small volume in the case of the "hourglass" geometry. We will show later, however, that this limitation does not apply to inhomogeneous fields from sources such as magnetite grains[16–19] which behave very differently and may have local frequency variations comparable to ω_0.

There are probably not many conical points on pore surfaces, but there are crystal corners which sometimes have sharp points and should give fields much like the cones. Crystal edges are often encountered in porous rocks. At a substantial distance from corners the system may locally be approximated by a wedge, giving a two-dimensional magnetic field problem. Using Fig. 1 now as representing a two-dimensional wedge and applying Eq. (3), we get

$$B_d=\frac{\chi_d B_0}{\pi}\left\{\ln\sqrt{1+2\xi\cos\vartheta+\xi^2}-\ln\xi-\tan^{-1}\left[\frac{\sin\vartheta}{\xi+\cos\vartheta}\right]+\sin^2\vartheta\left[\tan^{-1}\left[\frac{1+\xi\cos\vartheta}{\xi\sin\vartheta}\right]-\frac{\pi}{2}+\vartheta\right]\right\}$$

$$\approx\frac{\chi_d B_0}{\pi}(-\sin\vartheta\cos\vartheta\ln\xi-\vartheta\cos^2\vartheta+2\xi\cos^2\vartheta\sin\vartheta)\ . \tag{7}$$

In two dimensions the field on the z axis of Fig. 1 can be continued analytically to give the field off axis. The singular part of Eq. (7) gives the analytic function $\ln(\zeta)$ of the complex variable ζ. If we let $\zeta=\rho e^{i\varphi}$, then $\ln\zeta=\ln\rho+i\varphi$. Since we are interested in the z component of the field, we have simply $\mathrm{Re}(\zeta)=\ln\rho$. If $h_0=a/2$ (wedge edge equal half the pore radius), we have $z_0=a/110$. We repeat the worst-case computation for two dimensions, where the area element is proportional to $\rho d\rho$. With the same parameters as for three dimensions, we get a worst-case dephasing rate of about 0.3 $\sec^{-1}$. Again, the possible logarithmic singularities do not have practical importance, and we may regard fields as limited to about $\pm\frac{1}{2}\chi_d B_0$.

Equations (2) and (3) lend themselves to our visualizing some features of the magnetic fields when we note that only components of surfaces normal to $\mathbf{B}_0$ contribute to B_d. Furthermore, only changes of magnetic fields over distances of the order of a few times the one-dimensional diffusion distance $\sqrt{4D\tau}$ are relevant for spin-echo measurements. The inherent field inhomogeneity of most instruments would not be significant, and in particular, fields dependent on the external shape of a sample of magnetic susceptibility of magnitude $\ll1$ are not important. We are interested in contributions of surfaces in Eqs. (2) and (3) only within a few diffusion distances. The surfaces at great distances contribute only a very slowly varying field, the results of which are canceled in the echoes despite the diffusion. Note that cylindrical boundaries with edges parallel to $\mathbf{B}_0$ with arbitrary cross section, make no contribution to the integrals. Thus, if we regard our sample as an infinitely long cylinder parallel to $\mathbf{B}_0$, we have the geometry where only local surfaces contribute. Note also that, once the distance is a few pore spacings from the local surfaces contribute. Note also that, once the distance is a few pore spacings from the field point, the solid material is statistically fairly uniformly distributed in the solid angle, hence making no contribution to the field at the point in question. It should be noted that we cannot do the usual matching of normal $\mathbf{B}$ and tangential $\mathbf{H}$ fields at boundaries when we ignore variations in $\mathbf{H}$ of first order in χ_d.

With the conventions adopted above, we can list the fields in a few idealized pore shapes. First, related to the

discussion of sample shape, we note that a long thin cylindrical pore with axis parallel $\mathbf{B}_0$ has no additional field due to the susceptibility difference, as there is no contribution from the sides, and the ends are far away. The same would apply to a narrow crack with walls parallel $\mathbf{B}_0$. However, the additional field in a narrow crack normal to $\mathbf{B}_0$ is $\chi_d B_0$. The field surrounding a solid cylinder of radius a and axis normal to $\mathbf{B}_0$ is $B_d = \frac{1}{2}\chi_d B_0 (a/\rho)^2 \cos 2\varphi$, that of a two-dimensional dipole; the uniform field inside a cylindrical pore with axis normal to $\mathbf{B}_0$ is $B_d = \frac{1}{2}\chi_d B_0$. The dipole field surrounding a solid sphere is $B_d = \frac{1}{3}\chi_d B_0 (a/r)^3 (3\cos^2\vartheta - 1)$; the uniform field inside an isolated spherical pore is $B_d = \frac{1}{3}\chi_d B_0$ (with respect to field in the absence of the solid framework, not with respect to that in the solid).

A porous rock cannot easily have a solid sphere surrounded by fluid for large distances, but this can exist in a gel suspension. Furthermore, porous media made of various kinds of sphere packs are used for many purposes. For these, the field in the pore spaces is simply the sum of the fields of dipoles located at the centers of the spheres. As before, this simple relationship depends on $|\chi_d| \ll 1$. Some very high-porosity artificial porous media have some features that are somewhat like columns, or short cylinders. Most rocks do not have pores that are very nearly spherical, and furthermore, most pores have neighbors and are thus not isolated in an infinite medium. Nevertheless, special cases of these types give ideas about some of the properties of the fields. A pore that has dimensions in all three directions significantly larger than the scale of the surface roughness and of connecting channel diameters should have a significant region of relatively uniform field. Molecules starting in the middle of such a region would have to diffuse much longer to experience a change of field sufficient to interfere with echo formation than would molecules starting near sharply changing fields in channels, corners, edges, and smaller grains. We wish to get a rough idea of the ranges of local fields and diffusion times for significant change of local fields.

Equations (2) and (3) are particularly easy to interpret for a surface normal to $\mathbf{B}_0$, since, in two dimensions, the integrand of Eq. (3) is in this case simply the angle subtended from the field point by dy, and in three dimensions, the integrand of Eq. (2) is the element of solid angle subtended. Suppose we have a pore that has on one side a plane solid wall normal to $\mathbf{B}_0$ intersecting a wall parallel to $\mathbf{B}_0$. A molecule of fluid very close to the first wall, the wall contributing to B_d, sees wall through an angle of nearly π in two dimensions (or a solid angle of 2π in three dimensions). As the molecule is moved while remaining a fixed short distance from the wall to a point in line with the second wall (parallel $\mathbf{B}_0$ and hence not contributing to B_d) the angle subtended by the first wall is now only $\frac{1}{2}\pi$. If the point moves until it is in line with the first wall and a very short distance out from the second wall, the angle subtended by the first wall is zero. If now we move a distance along the second wall, the first wall subtends an angle of $-\frac{1}{2}\pi$. Thus, by going around the corner, the integral in Eq. (3) changes by an amount $\frac{3}{2}\pi$, so the change in B_d is $\frac{3}{4}\chi_d B_0$. By staying very close to the solid we have been able to go around the corner by moving only a very short distance, thus not changing distances to other surfaces significantly. However, if we wish to consider a significant amount of the liquid sample, and hence a significant amount of signal, we must include molecules of the liquid somewhat farther from the surfaces, and these must diffuse greater total distances, probably also changing distances to other contributing surfaces and probably also reducing the subtended angles somewhat. Many porous rocks contain crystals with sharp edges. We have numerous configurations that give the possibility for a fraction of the fluid molecules, under diffusion, to change field and precession frequency significantly in much shorter times than for parts of the fluid starting in other positions, such as in the centers of large pores.

In summary, field variations B_d in the pores of a porous medium where there is a susceptibility difference χ_d between components, such as between solid and fluid, may, for practical purposes, be regarded as roughly confined to the range $\pm\frac{1}{2}\chi_d B_0$ from the local mean values. Local mean values refer to values in pore spaces accessible by diffusion in time 2τ, where 2τ is the CPMG echo spacing. Significant changes in B_d occur over quite different correlation times for fluid molecules starting in different parts of a pore, and local fields may be different also. It may be that fields in the larger pores may, in some porous materials, have values closer to the mean (smaller $|B_d|$) and also have longer correlation times for molecular motion than some others. Our derivation in the next section will apply our finding that the diffusion of fluid molecules through the pore spaces leads spins to experience a limited range of precession frequencies but with the changes of frequency occurring over a substantial range of time scales for spins starting in different positions in the pore space.

APPROXIMATE COMPUTATION OF CPMG ECHO AMPLITUDES

The pore systems of many porous media are so complex that it is not possible to specify geometrical detail sufficiently for numerical computation, let alone for analytic computation, of CPMG echo train decay. We will use a model for computation which, under conditions to be discussed, appears to account for appropriate ranges of magnetic field variation and of times for changes of magnetic field experienced by molecules because of their diffusive motion. We assume that there is no applied macroscopic field gradient, and we ignore effects of residual gradients from the instrument because they would be canceled in a CPMG measurement, so would effects of sample shape and *macroscopic* variations in susceptibility. We start by considering properties of correlation functions for local variation ω of precession angular frequency, which is the frequency variation with respect to the local mean, and is hence a zero-mean variable. We will then use the correlation function to compute the mean-square phase dispersal $\langle \varphi^2 \rangle$ of the spins at time $2n\tau$, the time of the nth echo in a CPMG echo train. We then compute R_d as if the distribution of phases were Gauss-

ian, in which case decay is by a factor of

$$(2\pi\langle\varphi^2\rangle)^{-1/2}\int_{-\infty}^{\infty}\exp(-\tfrac{1}{2}\varphi^2/\langle\varphi^2\rangle+i\varphi)d\varphi = \exp(-\tfrac{1}{2}\langle\varphi^2\rangle)$$

(Ref. 20) and $R_d=\frac{1}{2}\langle\varphi^2\rangle/(2n\tau)$. We then try to see under what conditions this assumption gives reasonable results.

The correlation function is defined

$$F_{cc}(t,t')=\int\omega(t)\omega(t')dv = \langle\omega(t)\omega(t')\rangle=F_c(|t-t'|)\ ,$$

where dv is the fluid volume fraction, or fraction of spins. It depends only on $|t-t'|$ because in the diffusion there is no change in probabilities with time shift or reversal. It is not possible to specify the exact form of $F_c(|t-t'|)$, but it has the property of decaying to zero at long times, since ω is a zero-mean variable. We can represent a rather general function of this sort as a sum of decaying exponentials of the form $\exp(-|t-t'|/\tau_{ci})$, where the τ_{ci} are correlation times. An example of a system with a single correlation time would be two pores of the same size, with precession frequency uniform within each but different from each other and with loose coupling by diffusion between the two. A number of isolated such systems of different sizes will give a range of τ_{ci}; however, the porous media we are considering are not isolated systems. The fact that we represent F_c by a sum of exponential components in no way means that we merely have different noninteracting parts of the system with their own different correlation times. It also does not mean that the ω of a subset of spins starting at some time in one very small region are exponentially correlated in time with their future ω values; in fact, such correlations need not even be monotonically decreasing, although most probably are. Likewise it does not mean that the spins with a given τ_{ci} all start in the vicinity of some particular point. Rather, they may represent eigenstates of a diffusion equation in the pore system, usually too complicated for computation. Of course, if there are subregions, either macroscopic or microscopic, that do not communicate significantly by diffusion in measurement times, we will regard these regions as having their own separate computations of contributions to $\langle\varphi^2\rangle$. In this connection it should be noted, for instance, that diffusion in some visually homogeneous sandstones is not sufficient to prevent distributions even of T_1 (which involves longer times than T_2 and is not affected by the susceptibility differences) from extending over as much as three decades.[21,22]

Thus, we surmise, without proof, in order to show general properties of CPMG echo trains in many porous media, that F_c can be represented by a sum of exponential components which are all of the same sign and that there are substantial components over a range of the order of a decade or more in correlation times, giving a correlation function of the form

$$F_c=\sum_i v_i\Omega_i^2\exp(-|t-t'|/\tau_{ci})\ , \tag{8}$$

where v_i are the volume fractions and $\Omega_i=\langle\omega_i^2\rangle$ are the rms values of ω for v_i. We will use the correlation function to compute $\langle\varphi_i^2\rangle$. The contributions of the various exponential components in Eq. (8) are additive, so it will suffice to derive the contributions to $\langle\varphi^2\rangle$ of a single exponential component.

For each spin we find the phase shift at time $2n\tau$ by integrating its ω over a time τ (between the initial 90° pulse and the first 180° pulse), subtracting the integral from τ to 3τ, and alternately adding and subtracting phase shifts for intervals 2τ. The final interval is τ, ending at the time of the nth echo. The indicated averages are over all spins:

$$\langle\varphi^2\rangle=\left\langle\left[\int_0^{\tau}\omega(t)dt+\sum_{k=1}^{n-1}(-)^k\int_{(2k-1)\tau}^{(2k+1)\tau}\omega(t)dt+(-)^n\int_{(2n-1)\tau}^{2n\tau}\omega(t)dt\right]^2\right\rangle\ , \tag{9}$$

$$\begin{aligned}\langle\varphi^2\rangle=&\int_{t=0}^{\tau}\int_{t'=0}^{\tau}\langle\omega(t)\omega(t')\rangle dt\,dt'+\sum_{k=1}^{n-1}\int_{t=(2k-1)\tau}^{(2k+1)\tau}\int_{t'=(2k-1)\tau}^{(2k+1)\tau}+\int_{t=(2n-1)\tau}^{2n\tau}\int_{t'=(2n-1)\tau}^{2n\tau}\\&+2\sum_{k=1}^{n-1}(-)^k\int_{t=0}^{\tau}\int_{t'=(2k-1)\tau}^{(2k+1)\tau}+2\sum_{k=1}^{n-1}(-)^{n\pm k}\int_{t=(2n-1)\tau}^{2n\tau}\int_{t'=(2k-1)\tau}^{(2k+1)\tau}\\&+2(-)^n\int_{t=0}^{\tau}\int_{t'=(2n-1)\tau}^{2n\tau}+2\sum_{k=1}^{n-2}\sum_{l=k+1}^{n-k-1}(-)^l\int_{t=(2k-1)\tau}^{(2k+1)\tau}\int_{t'=[2(k+l)-1]\tau}^{[2(k+l)+1]\tau}\ ,\end{aligned} \tag{10}$$

where all integrands are $\langle\omega(t)\omega(t')\rangle dt\,dt'$. In each integral $\langle\omega(t)\omega(t')\rangle=\Omega^2e^{-|t-t'|/\tau_c}$.

To save writing, we will express t, t', and τ in units of τ_c. The first and third integrals in Eq. (10) are the same by time reversal and will each be called $I_{0,0}\Omega^2\tau_c^2$. The first sum of integrals will be called $2I_{k,k}\Omega^2\tau_c^2$. These represent the squared terms in Eq. (9). The cross terms all have factors of 2 if they are restricted to having the second index larger than the first. The first cross term is between the first and last intervals, which have widths of τ instead of 2τ, and it will be called $I_{0,n}\Omega^2\tau_c^2$. The two single sums among the cross terms are identical by time reversal and will each be called $\frac{1}{2}I_{0,k}\Omega^2\tau_c^2$. The double sum will be called $I_{k,k+l}\Omega^2\tau_c^2$. We now have

$$\Phi=\frac{\langle\varphi^2\rangle}{2\Omega^2\tau_c^2}=I_{0,0}+I_{k,k}+I_{0,n}+I_{0,k}+I_{k,k+l}\ . \tag{11}$$

The τ_c^2 in the denominator comes from putting dt and dt' in units of τ_c. We have

$$I_{0,0}==\int_{t=0}^{\tau}dt\left[\int_{t'=0}^{t}e^{+(t'-t)}dt'+\int_{t'=t}^{\tau}e^{-(t'-t)}dt'\right]$$
$$=2\tau-2+2e^{-\tau}\ , \tag{12}$$

$$I_{k,k}=(n-1)(2\tau-1+e^{-2\tau})\ , \tag{13}$$

$$I_{0,n}=(-)^n\int_{t=0}^{\tau}dt\int_{t'=(2n-1)\tau}^{2n\tau}e^{-(t'-t)}dt'$$
$$=(-)^n(1-e^{-\tau})^2e^{-2(n-1)\tau}\ . \tag{14}$$

$I_{0,k}$ is a geometric series and can be summed,

$$I_{0,k}=-2\frac{(1-e^{-\tau})(1-e^{-2\tau})}{1+e^{-2\tau}}$$
$$\times[1+(-)^ne^{-2(n-1)\tau}]\ . \tag{15}$$

The integral $I_{k,k+l}$ is a double sum,

$$I_{k,k+l}=\sum_{k=1}^{n-l-1}\sum_{l=k+1}^{n-k-1}(-)^l\int_{t=(2k-1)\tau}^{(2k+1)\tau}dt\int_{t'=[2(k+l)-1]\tau}^{[2(k+l)1]\tau}e^{-(t'-t)}dt'\ . \tag{16}$$

The terms with equal l values are equal, giving us the single sum,

$$I_{k,k+l}=\sum_{l=1}^{n-l-1}(n-l-1)(-)^l\int_{t=-\tau}^{\tau}dt\int_{t'=(2l-1)\tau}^{(2l+1)\tau}e^{-(t'-t)}dt'\ . \tag{17}$$

Doing the sums and gathering terms,

$$I_{k,k+l}=(1-e^{-2\tau})^2\left[-\frac{n-1}{1+e^{-2\tau}}\right.$$
$$\left.+\frac{1+(-)^ne^{-2(n-1)\tau}}{(1+e^{-2\tau})^2}\right]\ . \tag{18}$$

Putting Eqs. (12)–(15) and (18) in Eq. (11), we have, with considerably more gathering of terms,

$$\Phi=\frac{\langle\varphi^2\rangle}{2\Omega^2\tau_c^2}=2n\tau\left[1-\frac{\tanh(\tau)}{\tau}\right]$$
$$+\frac{(1-e^{-\tau})^4}{(1+e^{-2\tau})^2}[-1+(-)^ne^{-2n\tau}]\ . \tag{19}$$

It is worth noting results for some special values of n. Equation (18) for $I_{k,k+l}$ was derived assuming that $n>2$, but we note that it is zero for $n=1$ or 2. Likewise, Eq. (13) for I_{kk} and Eq. (15) for $I_{0,k}$ were derived assuming that $n>1$, but we note that they are zero for $n=1$. In addition, we may note from Eq. (19) that $\Phi=0$ for $n=0$. For single spin echoes instead of CPMG echo trains we get for $n=1$,

$$\Phi=2\tau-(1-e^{-\tau})(3-e^{-\tau})$$
$$=2\tau\left[1-\frac{3-4e^{-\tau}+e^{-2\tau}}{2\tau}\right]\ . \tag{20}$$

For very small τ, Eqs. (19) and (20) have the same behavior, namely as $\tau^2/3$. For large τ Eq. (20) goes as $2\tau-3$ (still in units of τ_c). That is, the observed additional relaxation would be

$$\text{(single echoes)}\quad R_d=\Omega^2\tau_c \tag{21}$$

if measurements are made only at times much longer than τ_c. The spin density would be overestimated by a factor of $\exp(3R_d\tau_c)$.

For CPMG data we note that the term in Eq. (19) containing the factor $e^{-2n\tau}$ is both small and also much smaller than the term with the factor $2n\tau$ and that the term not involving n merely causes a shift in the decay curve. This shift would lead us to overestimate the spin density by a factor of

$$\exp[(1-e^{-\tau})^4(\Omega\tau_c)^2/(1+e^{-2\tau})^2]\ ,$$

again, with τ still in units of τ_c. Therefore, R_d can be well approximated by

$$\text{(CPMG)}\quad R_d=\Omega^2\tau_c\left[1-\frac{\tanh(\tau)}{\tau}\right]\ . \tag{22}$$

We now drop the convention of specifying times in units of τ_c and consider $\langle\varphi^2\rangle$ resulting from several correlation times or a distribution of times. If v_i is the fraction of the spins contributing to the ith mode, we get

$$R_d=\sum v_i\Omega_i^2\tau_{ci}f(\tau/\tau_{ci})\ ,$$
$$f(\tau/\tau_{ci})=1-\frac{\tanh(\tau/\tau_{ci})}{\tau/\tau_{ci}}\ . \tag{23}$$

Thus, assuming for the present that the φ distribution is close enough to Gaussian and that relaxation is close enough to single exponential, $R_d(\tau)$ is given by Eq. (23). Curve a of Fig. 2 shows $f(\tau/\tau_c)$, which starts out quadratically and has a fairly long, nearly straight, section. Curve b of Fig. 2 is

$$\{f(\tau/\tau_c)+0.1f[\tau/(0.1\tau_c)]\}/1.1\ ,$$

which is equivalent to components a factor of 10 apart in τ_c with the same $v_i\Omega_i^2$ product, with the curve normalized to the same asymptotic value. This curve also, of course, starts out quadratically, but on the scale of this plot it appears nearly linear to about 45% of its asymp-

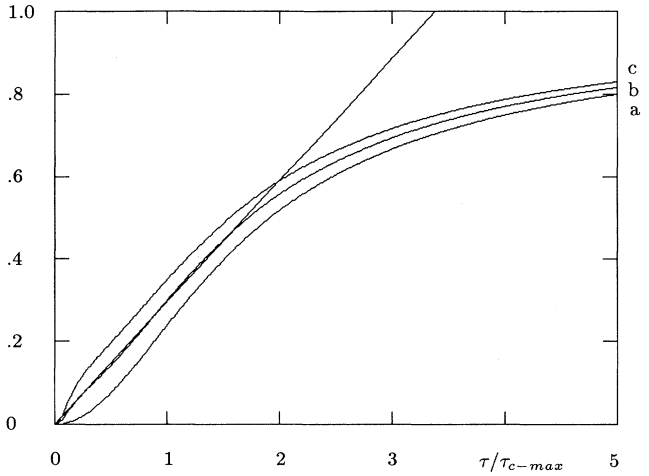

FIG. 2. Curve a is $f(t)=1-(\tanh t)/t$, where $t=\tau/\tau_c$, corresponding to R_d for a single correlation time. Curve b is $[f(t)+0.1f(10t)]/1.1$, corresponding the contribution to R_d of equal numbers of spins (times mean-square frequency variation) with $\tau/\tau_c=t$ and with $t/\tau_c=10t$, normalized to unit asymptote for large t. The coefficient is proportional to τ_c. Curve c is $[f(t)+0.2f(10t)]/1.2$ corresponding to twice the short component.

totic value. Curve c shows the result of doubling the short-τ_c component. This "overcorrects" for the slow start of $f(\tau/\tau_c)$.

We find that many sums of the form of Eq. (23) have nearly constant slope for small τ, and that all such sums and distributions have slopes proportional to $1/\tau^2$ for large τ. These features can be conveniently combined in the function $1/(1+\tau^2)$, which is the derivative of the arctangent function. We will compare this function with both some sums and distributions of functions $f(\tau/\tau_{ci})$ and also with sets of experimental data.

In Fig. 3, all curves are normalized to unit asymptote and have the value of 0.25 at unit abscissa. Curve a of Fig. 3 is otherwise the same as curve b of Fig. 2. Curves b and c of Fig. 3 are sums of 11 components equally spaced in log time and spanning a correlation time ratio of 100. The components have equal $\Omega_i^2 v_i$ products except for the end points. For curve b the end weighting is threefold, and for curve c the end weighting is half. It may be noted that the stronger end weighting gives a longer nearly linear region. A fourth curve, shown by solid circles instead of solid lines, is the arctangent function, similarly normalized. A straight line with slope 0.25 is shown for reference. It can be seen that a considerable variety of distributions of τ_c's can give substantial initial portions of the curves that are nearly linear.

Figure 4 shows the dependence of R_d on $\tau_{c\text{-gm}}$, the geometric-mean correlation time, for four different distributions of τ_c's. Curve a is for a single τ_c, curve b is for the pair of τ_c's of curve b of Fig. 2 or curve a of Fig. 3, curve c corresponds to curve b of Fig. 3, and the curve shown by $\times$'s to avoid confusion with curve c corresponds to curve c of Fig. 3. Note that all but curve a have significant regions that are relatively flat. For these a small change of diffusion coefficient D of the fluid would have minimal effect on R_d if $\tau_{c\text{-gm}}$ starts in the flat region. The correlation times should vary inversely as D, which can be changed by changing temperature or by

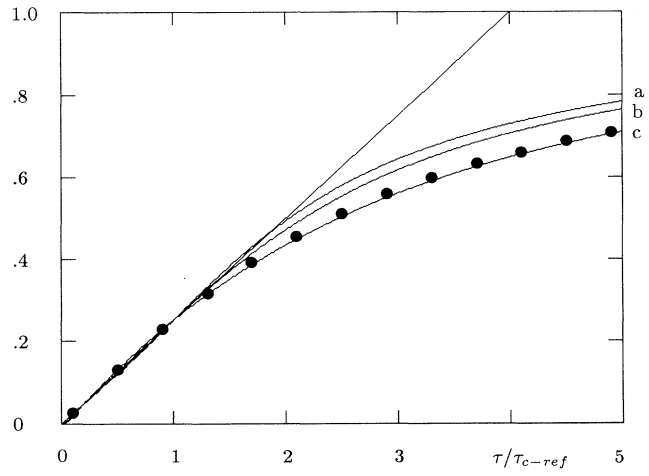

FIG. 3. All curves are normalized to unit asymptote and to be equal to 0.25 at unit abscissa. Curve a is otherwise the same as curve b of Fig. 2. Curve b and c correspond to sums of 11 terms with τ_c values equally spaced in $\log_{10}(\tau_c)$ over a factor of 100, with equal $\Omega_i^2 v_i$ products, except that the end points for curve b have threefold weight and the end points for curve c have half-weight. The curve shown by solid circles is the arctangent function, similarly normalized. A straight line with slope 0.25 is shown for reference. The above normalization determines $\tau_{c\text{-ref}}$, the reference value for τ_{ci}.

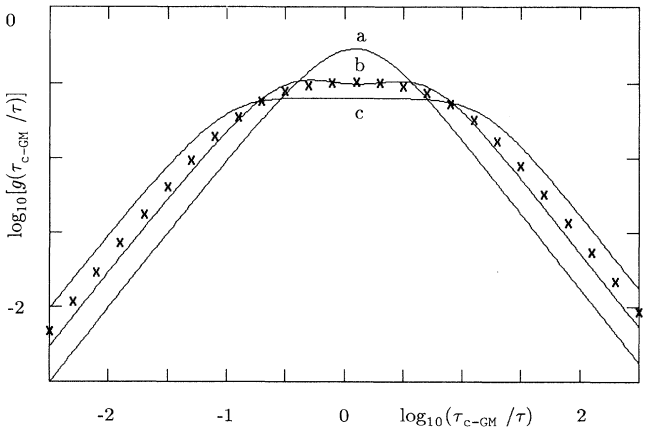

FIG. 4. The curves plotted are proportional to the dependence of R_d on τ_c for fixed τ. For the distributions $\tau_{c\text{-gm}}$ refers to the geometric mean τ_c. Curve a is $g(t)=tf(2/t)$, where $t=\tau_c/\tau$, and the factor of 2 (using a ratio of correlation time to echo time 2τ rather than to τ) is for near symmetry on the log plot. Curve a thus represents a single correlation time. Curve b corresponds to curve a of Fig. 3 or curve b of Fig. 2. Curve c corresponds to curve b of Fig. 3 (stack with threefold end weighting), and the $\times$'s correspond to curve c of Fig. 3 (half-weight for ends). In the nearly flat areas R_d is not sensitive to small changes in correlation times, as from change of fluid or of temperature.

changing the fluid. The region of minimal dependence of R_d on $\tau_{c\text{-gm}}$ is the region of nearly linear dependence on τ. The above shows that such combinations or distributions of correlation times over a decade or more tend to give quasilinear τ dependence of R_d for small τ.

DISCUSSION AND EXAMPLES

Many porous media containing fluids are subject to precession angular frequency differences, which for practical purposes are limited to a range of about $\pm\frac{1}{2}\chi_d\omega_0$. Furthermore, there are different porespace regions in close proximity where diffusion leads to changes of local ω over quite different time scales or correlation times. The distribution of correlation times leads to a mean-square phase dispersal $\langle\varphi^2\rangle$ at the time of the nth CPMG echo, that is, for small τ, roughly quadratic in τ rather than cubic as for unbounded diffusion in a uniform field gradient. This corresponds to a roughly linear rise of R_d with τ for small τ. If the distribution in φ is Gaussian, the normalized echo amplitude is

$$S=\exp(-\tfrac{1}{2}\langle\varphi^2\rangle)\ , \tag{24}$$

a relationship we have already used. If $\langle\varphi^2\rangle$ that accumulates in regions of short τ_c is not large at time 2τ and has time to spread to regions of longer τ_c in time $2n\tau$, the increment to $1/T_2$ from the inhomogeneous fields from susceptibility differences is reasonably approximated by $R_d=\frac{1}{2}\langle\varphi^2\rangle/(2n\tau)$.

The special nature of the properties of the magnetic fields described above can be made clearer by an important example of locally inhomogeneous fields with quite different properties. In areas as diverse as oil well logging[1] and medical magnetic resonance imaging, magnetic grains such as magnetite grains have been used as contrast agents to decrease the transverse relaxation times T_2. Hardy and Henkelman[17,18] (HH) and Muller *et al.*[19] have done Monte Carlo calculations for CPMG echoes to find the dependence of R_d on grain size, concentration, dipole moment, diffusion coefficient D, and τ. HH find best fits to their computations with R_d proportional to $D^{0.9}$ and to $\tau^{0.6}$. In the present problem D is inversely related to correlation times, which over a substantial range are shown, however, to have relatively little effect on R_d. The τ dependence for CPMG with the magnetic grains is even further from the traditional τ^2 dependence than the linear dependence discussed in the present paper. HH point out that in their cases it is not sufficient to compute second moments of phases distributions $\langle\varphi^2\rangle$ because the distributions are not known *a priori* and are not close to Gaussian. They have a sharp central peak and broad tails and can have the same second moment as a Gaussian which gives a very different R_d.

The phase distribution for free precession signal decay or for magnetic resonance imaging (MRI) gradient echo decay due to magnetic grains is even more extreme than for CPMG. Brown[16] has shown that in the field of randomly distributed point dipoles the phase distribution is of the Cauchy form, which does not even have a finite second moment. Here, an analytic expression is given for the contribution of the grains to R_d, which, quite remarkably, does not depend on D at all. In this specific system the frequency averaging from diffusion is exactly offset by the "hazard" of coming close to the very strong field of a point dipole. This feature is what sets the dipole problem apart from our present problem, where the effective frequency range is limited to compact distributions without long tails.

It is clear that the present paper does not apply to cases where compact magnetic grains are present. However, the scope can be extended somewhat to include some paramagnetic materials imbedded in the solid phase of the porous material. Some smooth magnetic coatings might also fit the conditions of the present work, but the limited frequency range from the inhomogeneous fields is essential to the present problem. It is not essential to the considerations of this paper that χ_d be constant over the medium or even everywhere of the same sign, but we require $|\chi_d|\ll 1$. Diamagnetic susceptibility should not have significant temperature dependence, but paramagnetic susceptibility usually follows the Curie-Weiss law. Thus, a temperature increase could decrease χ_d, thereby decreasing Ω, and would also increase D, thereby decreasing the τ_c's related to diffusion.

We have shown that porous media can have substantial ranges of correlation times, and we have computed $\langle\varphi^2\rangle$ for some specific distributions. We do not in this paper attempt to evaluate any specific model of porespaces, but it is necessary to discuss conditions for $\langle\varphi^2\rangle$ to be related to R_d as for a Gaussian distribution in φ. There are several ways a distribution might be qualitatively different from Gaussian. We do not see how to get a bimodal distribution or rectangular distribution of echo phases from diffusion through a range of frequencies. Distributions resulting from repeated contributions from compact distributions, even with alterations by diffusion and repeated refocussing, should tend toward Gaussian.[20] We have already discussed the distributions with extended tails being excessive in the sense that very large phase shifts at echo time are experienced by small numbers of spins. These large phase shifts do not reduce the signal any more than moderate shifts, but they make inordinate contributions to $\langle\varphi^2\rangle$.

A condition for not having excessive contributions to $\langle\varphi^2\rangle$ in time 2τ is that there not be significant local regions with $|\varphi|\gg 1$ rad. This requires that the overall echo decay by much less than 1 Np. Another way of saying this is that there should be a substantial number of echoes in time T_2. Our measurements at 20 MHz suggest that about seven echoes in time T_2 are required for the quasilinear τ dependence to apply.

The above argument can be given slightly more quantitatively by considering at any echo time a distribution of phases which is a sum of Gaussians with amplitudes A_i and half-widths σ_i. This can represent the above situation where a large contribution to $\langle\varphi^2\rangle$ can come from a small fraction of the signal. If $\sum A_i=1$ then $\langle\varphi^2\rangle=\sum A_i\sigma_i^2$. The echo amplitude S is now

$$S=\sum A_i\exp(-\tfrac{1}{2}\sigma_i^2)\approx\exp\left[-\frac{1}{2}\sum A_i\sigma_i^2\right] \tag{25}$$

if σ_i are small. For the tissue and porous media cases that we are discussing, the limited range of $|\omega|$ gives the possibility for $\sigma_i < 1$ if Ω^2 is not too large. For measurements on tissues, rocks, and artificial porous media at 20 MHz these conditions seem to be satisfied just about to the end of the straight portion of Fig. 3. At much higher frequencies, and hence higher Ω^2, the failure of Eq. (25) should cause the quasilinear portion of R_d vs τ to end before the end of the quasilinear behavior of curve b of Fig. 2. For much lower frequencies R_d is much smaller, but Eq. (25) should apply, and R_d should roughly follow the pattern of Fig. 3.

Most porous media have spins with a range of correlation times for spins diffusing in the porespaces in such a way that mixing throughout the system may be limited in time 2τ but substantial in time $2n\tau$. This mixing corresponds to a summing of samples from a distribution which is not Gaussian but which does not have long tails. These sums tend toward Gaussian distributions, leading to the validity of Eq. (24). As already mentioned, these communicating and mixing sets of spins with a range of τ_c's may be a subset of all spins in a complicated sample such as a rock with a wide range of relaxation times. It should be noted that different measurements, such as T_1 or such as T_2 by CPMG with different τ's, on a given sample can give very different relaxation times and hence different ranges of mixing by diffusion.

We now compare the behavior shown in Figs. 2–4 with experimental results for T_1, T_2 from Hahn single echos, and T_2 from CPMG echo trains at 25 °C and 41 °C at 20 MHz. Details of sample preparation and NMR measurements are published elsewhere.[8,23]

Figures 5 and 6 are plots for an artificial porcelain sample of uniform pore diameter[23] of the order of a few μm. Discrete multicomponent relaxation fits were made with

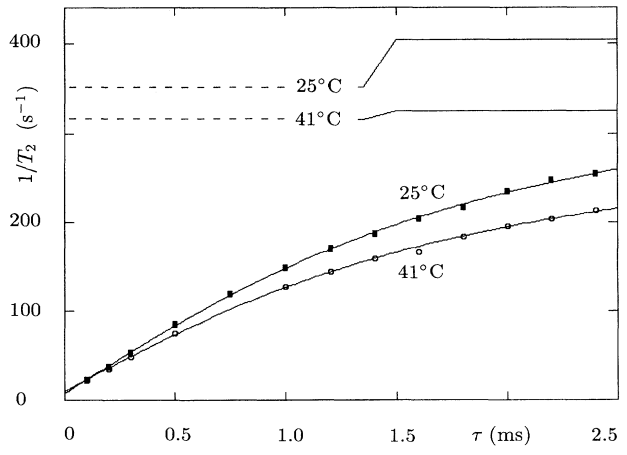

FIG. 5. Experimental $1/T_2$ values from CPMG measurements as a function of τ for water in an artificial porcelain sample at 25 °C and 41 °C. The solid curves are the arctangent fits, and the solid horizontal lines are the asymptotes. The dashed horizontal lines are the $1/T_2$ values from the nearly single exponential portions of Hahn single-echo data, presumably for times longer than prominent correlation times.

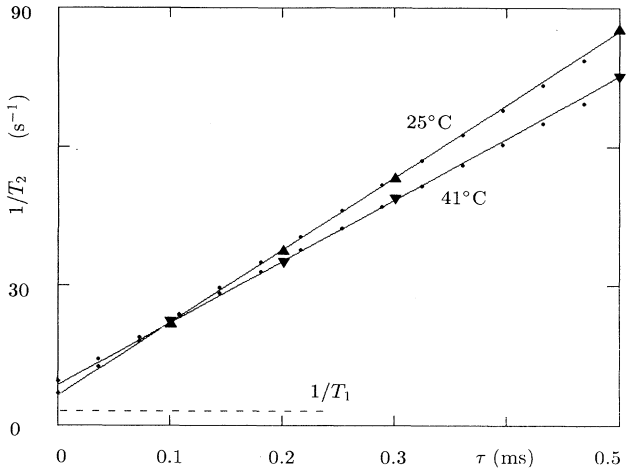

FIG. 6. Expanded plot of the first four points of Fig. 5. The solid lines are linear regression fits to the first four points, and the equally spaced dots are the same arctangent fit to the entire data set as shown in Fig. 5. The dashed line near the bottom is the mean of the $1/T_1$ values for the two temperatures. The separate $1/T_1$ values would be barely resolvable on the scale of the plot.

signal value at infinite time as a regression variable and with as many exponential components as improved the standard error of fit without amplitudes of different signs or relaxation times outside the range covered by the data. T_1 was single exponential for both temperatures. At 25°, $T_1 = 327$ msec and at 41° $T_1 = 360$ msec. Correction for bulk water relaxation times[24] changes these only to 360 and 388 msec, respectively. Thus, the surface effect for T_1 varies in the "normal" direction with temperature. The logarithms of the Hahn single-echo decay curves showed straight-line portions after 3 msec, corresponding to $T_2 = 2.8$ msec at 25° and $T_2 = 3.2$ msec at 41°.

The CPMG data for the several shortest-τ points gave substantially the same values of S_0, the signal extrapolated to zero time, and this point was added as a point to the longer-τ data sets, stabilizing these T_2 computations considerably, since for the longer τ 's 2τ can be longer than T_2. The extrapolated signals were nearly the same for several τ values, confirming that the terms in Eq. (19) without the factor $2n\tau$ do not significantly distort the ratio of S_0 to the later data points. Adding the extrapolated zero points is useful for our samples because there are narrow distributions of relaxation times. Otherwise, there is excessive detail between the point at time zero and the next data point and no information to supply this when 2τ is large.

Nearly all of the CPMG relaxation curves yielded two components. The few that got three showed only slight improvement in fit with the third. The standard error of fit relative to the relaxing amplitude was 0.4%. The two-component fit for $\tau = 0.1$ msec at 25° was 87% at 57 msec and 13% at 8.6 msec. For plotting a single-parameter T_2 vs τ we have used the two-component geometric mean, namely, $\exp(\sum p_i \ln T_i)$, where p_i are the signal fractions. When the deviation from single ex-

ponential behavior is mild, as it is here, various kinds of "averages" can be used, such as geometric mean, single-component fit, the $1/e$ value, or the stretched exponential, but when there is substantial deviation from single exponential the different averages give quite different results.

Figure 5 shows the two-component geometric mean relaxation rates for various τ's and the two temperatures. The solid curves are nonlinear regression fits to the arctangent

$$1/T_2 \approx R_a + R_b \tan^{-1}(R_c\tau) \ . \tag{26}$$

The initial slopes are $\psi = R_a R_b$. The horizontal solid lines in Fig. 5 are the asymptotes $R_a + 2B_b/\pi$, and the horizontal dashed lines are the Hahn single-echo values of $1/T_2$. The agreement is good considering amount of the extrapolation and the fact that the single-echo data could be used only after several msec. It is not possible to carry the data meaningfully out to much larger τ's to approach the asymptotes more closely, as 2τ is greater than T_2.

Figure 6 shows an expanded plot of the nearly linear portion of Fig. 5, with four well-spaced experimental points very close to a straight line for each temperature, showing slopes $\psi(25\,^\circ) = 0.156$ (msec)$^{-2}$ and $\psi(41\,^\circ) = 0.133$ (msec)$^{-2}$. The straight lines are linear regression fits to the four points only, and the equally spaced dots show the same arctangent functions fit to the entire data sets as shown in Fig. 5. The arctangent fits gave essentially the same values of ψ and only very slightly lower values of the $\tau \rightarrow 0$ intercept.

For unbounded diffusion in a uniform gradient the rate is proportional to the diffusion coefficient D, and for diffusion in the vicinity of magnetic grains, HH (Refs. 17 and 18) found proportionality to about $D^{0.9}$. For water[25] $D(25\,^\circ) = 2.590$ $(\mu\text{m})^2$/msec and $D(41\,^\circ) = 3.793$ $(\mu\text{m})^2$/msec, a ratio of 1.46. The mechanisms discussed in the present paper suggest minimal dependence on the τ_c's for the region of nearly linear τ dependence, and we assume that the τ_c's correlate inversely with D. For the sample of Figs. 5 and 6 we have weak dependence on D in the opposite sense, with a higher rate at the lower temperature. This probably indicates that we are on the long-τ_c side of one of the curves of Fig. 4, leaving somewhat less short-τ_c contribution at 25° than at 41°. If we are in the "undercorrected" regime, between curves a and b in Fig. 2, the extrapolation could deviate from τ linearity at very small τ, probably with a larger deviation for the 25° curve. In Fig. 6, the two curves cross at $\tau \approx 0.1$ msec, and the intercepts correspond to $T_2 = 160$ msec at 25° and 115 msec at 41°. However, the extrapolation is in this case severe, about three times the lower intercept, and it is probably not reliable to use the τ-linear model to infer the difference between the "true" T_2's, the values due to surface and bulk effects without the susceptibility differences. The intercepts are, as they must be, somewhat higher than the values of $1/T_1$, the mean of which is shown as a dashed line near the bottom of Fig. 6.

Figure 7 shows data for a highly homogeneous natural porous chalk sample, with pore diameter in the range from 0.1 μm to 1μm, saturated with water. The T_1 com-

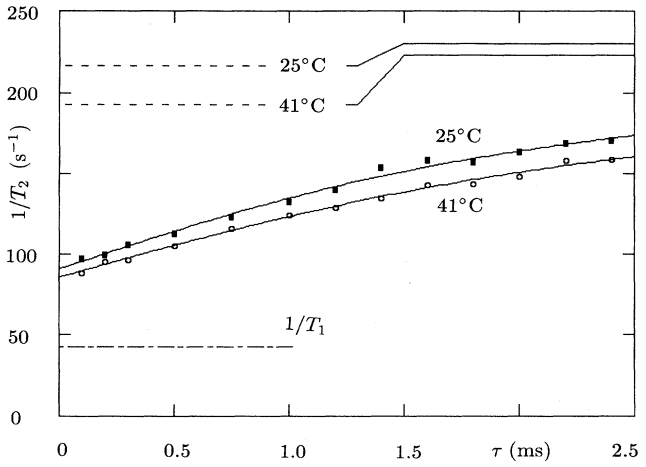

FIG. 7. Experimental $1/T_2$ values from CPMG measurements as a function of τ for water in a chalk sample at 25 °C and 41 °C. The solid curves are the arctangent fits, and the solid horizontal lines are the asymptotes. The horizontal dashed lines are the single-echo values of $1/T_2$. The horizontal long and short dashes show $1/T_1$, which is the same at both temperatures.

putations at the two temperatures were substantially identical and show two components, 8% at 100 msec and 92% at 21 msec. The two-component geometric mean $1/T_1$ is shown by the horizontal line of long and short dashes. Three-component fits were obtained to the CPMG data, but, for the sake of robustness, two-component geometric mean rates are plotted in Fig. 7. The fits at $\tau = 0.1$ msec are 25°: 6% at 44 msec, 84% at 10.6 msec, 10% at 3.0 msec; and 41°: 5% at 47 msec, 84% at 11.5 msec, 11% at 3.5 msec. Because of these 10% short components we used data only at multiples of 2.4-msec echo time in computing rates for $\tau = 0.1$, 0.2, and 0.3 msec, giving the same amount of detail in the three cases and hence making rate comparisons on an equal basis. Otherwise, even fairly narrow distributions of relaxation rates can lead to a sampling of longer relaxation times for a longer τ. Like the previous sample, the chalk shows only mildly non-single exponential relaxation. However, unlike the previous sample, the values of $1/T_2$ extrapolated to $\tau = 0$ are high. The solid curves in Fig. 7 are the arctangent fits, and the asymptotes are shown by the solid horizontal lines. The dashed horizontal lines are the values of $1/T_2$ from single-echo data.

The slopes ψ are nearly the same for the two temperatures and are an order of magnitude less than for the previous sample, with $\psi = 0.040$ (msec)$^{-2}$. Here the inhomogeneous field effect depends less on temperature, and hence on D or τ_c, than for the sample of Figs. 5 and 6. There is not much doubt about the relatively small extrapolation to the $\tau = 0$ intercept, which is about 9% higher at 25° than at 41°, whereas the T_1's are the same. For water[24] the rate is 43% higher at the lower temperature.

Jerosch-Herold, Thomann, and Thompson[4] have plotted T_2, rather than $1/T_2$ vs τ and fit the data with an ex-

ponential decaying from a T_2 intercept to a lower asymptote. We have scaled and replotted the points on one of their published curves to show $1/T_2$ vs τ, and we find the substantial linear portion similar to that shown in our Fig. 3. Their theoretical model, however, assumes uniform gradients in individual pores.

A tentative illustration of the significance of the limitation of the frequency variation ω to a limited range can be taken from work on experimental use of fine magnetite particles as a contrast agent in biological tissues. Rozenman, Zou, and Kantor[13] have shown T_2 data as functions of τ for several tissues which have taken up the particles. We have scaled and replotted their data with $1/T_2$ vs τ, finding dependence roughly as $\sqrt{\tau}$ or even $\sqrt[3]{\tau}$ except for the plot for liver, which shows initial linear τ dependence. This suggests that in the liver most water molecules cannot come very close to the magnetic grains; thus, the field experienced by the spins is limited. Indeed, the magnetic particles have been observed in phagosomes and secondary lysosomes of Kupffer cells, but not in any other cell type in the liver.[26]

Bendel[7] has made T_2 measurements for two τ values on samples with much larger pores than fit the assumptions of the present work. With the large pores the fast diffusion regime applies to the T_1 data, but the slow diffusion applies to the T_2 data, because T_2 is greatly shortened by the effect of differences in susceptibility. This gives a significantly non-single exponential behavior for T_2.

CONCLUSIONS

Fluids in several kinds of porous systems have shown nearly linear τ dependence at small τ values for CPMG multiecho measurements of $1/T_2$. The arctangent function has provided a good fit to a number of sets of CPMG data over the entire available measurement ranges, and the asymptotes of the arctangent function have agreed satisfactorily with the values of $1/T_2$ from Hahn single-echo measurements. These features appear to be compatible with the existence of a limited range of local precession frequencies due to susceptibility differences between components of the system and the existence of a significant range of correlation times associated with the diffusion of molecules through various values of local field. Precautions are needed in the data taking and data processing of CPMG T_2 data to ensure that the same time ranges are adequately covered for different τ values.

ACKNOWLEDGMENTS

This work was supported by Italian MURST and CNR grants.

[1]R. J. S. Brown and B. W. Gamson, Trans. Soc. Pet. Eng. AIME **219**, 201 (1960).
[2]J. Zhong and J. C. Gore, Mag. Reson. Med. **19**, 276 (1991).
[3]R. L. Kleinberg and M. A. Horsfield, J. Mag. Reson. **88**, 9 (1990).
[4]M. Jerosch-Herold, H. Thomann, and A. H. Thompson (unpublished).
[5]S. Majumdar and J. C. Gore, J. Mag. Reson. **79**, 41 (1988).
[6]C. R. Fisel, J. L. Ackerman, R. B. Buxton, and T. J. Brady, Mag. Reson. Med. **17**, 336 (1991).
[7]P. Bendel, J. Mag. Reson. **86**, 509 (1990).
[8]G. C. Borgia, R. J. S. Brown, P. Fantazzini, and E. Mesini, Il Nuovo Cimento D **14**, 745 (1992).
[9]R. W. Bowtell, G. D. Brown, P. M. Glover, M. McJury, and P. Mansfield, Philos. Trans. R. Soc. London Ser. A **333**, 457 (1990).
[10]P. T. Callaghan, J. Mag. Reson. **87**, 304 (1990).
[11]H. Y. Carr and E. M. Purcell, Phys. Rev. **94**, 639 (1954).
[12]S. Meiboom and D. Gill, Rev. Sci. Instrum. **29**, 688 (1958).
[13]Y. Rozenman, X. Zou, and H. L. Kantor, Mag. Reson. Med. **14**, 31 (1990).
[14]P. Le Doussal and P. Sen, Phys. Rev. B **46**, 3465 (1992).
[15]G. E. Santyr, R. M. Henkelman, and M. J. Bronskill, J. Mag. Reson. **79**, 28 (1988).
[16]R. J. S. Brown, Phys. Rev. **121**, 1379 (1961).
[17]P. A. Hardy and R. M. Henkelman, Mag. Reson. Imag. **7**, 265 (1989).
[18]P. A. Hardy and R. M. Henkelman, Mag. Reson. Med. **17**, 348 (1991).
[19]R. N. Muller, P. Gillis, F. Moiny, and A. Roch, Mag. Reson. Med. **22**, 178 (1991).
[20]C. H. Neuman, J. Chem. Phys. **60**, 4508 (1974).
[21]R. J. S. Brown, G. C. Borgia, P. Fantazzini, and E. Mesini, Mag. Reson. Imag. **9**, 687 (1991).
[22]G. C. Borgia, P. Fantazzini, and E. Mesini, Mag. Reson. Imag. **8**, 435 (1990).
[23]G. C. Borgia, P. Fantazzini, G. Fanti, E. Mesini, L. Terzi, and G. Valdrè, Mag. Reson. Imag. **9**, 695 (1991).
[24]R. J. S. Brown, J. Phys. Chem. **73**, 3157 (1969).
[25]H. R. Pruppacher, J. Chem. Phys. **56**, 101 (1972).
[26]P. Gehr, J. D. Brain, S. B. Bloom, and P. A. Valberg, Nature **302**, 336 (1983).